Numerical analysis of geosynthetic reinforced piled embankment scale model tests

Ir. Theresa den Boogert, TU Delft (now Mobilis), Ing. Piet van Duijnen, Mobilis and Ir. Suzanne van Eekelen, Deltares/TU-Delft
Foto: Project N210, Huesker

Piled embankments with geosynthetic reinforcement are applied on soft soils and have several advantages. For example, the piled embankment can be constructed rather fast and has a small settlement after construction or is even settlement-free. Another advantage is that a piled embankment can be built next to sensitive constructions. A piled embankment consists of a field of piles with pile caps. On top of that, one or more layers of geosynthetic reinforcement (GR) are applied. On top of the GR the embankment can be constructed.

In 2010 the Dutch design guideline, CUR226 (2010), for the design of piled embankmenst was published. To validate the guideline, several field tests have been performed. From the field measurements it has been concluded that the design method is rather conservative. Improving the design guideline would reduce the construction costs of piled embankments. To understand the physical behaviour of the piled embankment and to validate design models, experimental scale tests have been performed by Deltares in partnership with Huesker, Naue, TenCate and Tensar. The results of the scale tests were analysed and published by Van Eekelen, et al. (2011a, 2011b and 2011c).

Plaxis simulations of the test series were performed to improve the understanding of the arching mechanism in the piled embankment, and where possible, to confirm the conclusions from the analysis of the scale tests. The simulations are part of the master thesis performed by Den Boogert (2011).

First the definition of the load distribution in the embankment will be presented. The scale tests are described in the second paragraph. Then the content of the finite element model is discussed. The results of the finite element model are analysed and compared to the results of the scale test. The paper ends with conclusions and recommendations.

Definition of load distribution

The vertical load on the piled reinforced embankment is distributed to the soft subsoil in three load parts: A, B and C (shown in figure 1). The load parts are defined by: part A is transferred directly to the piles by arching, part B is transported via the GR to the piles, and load

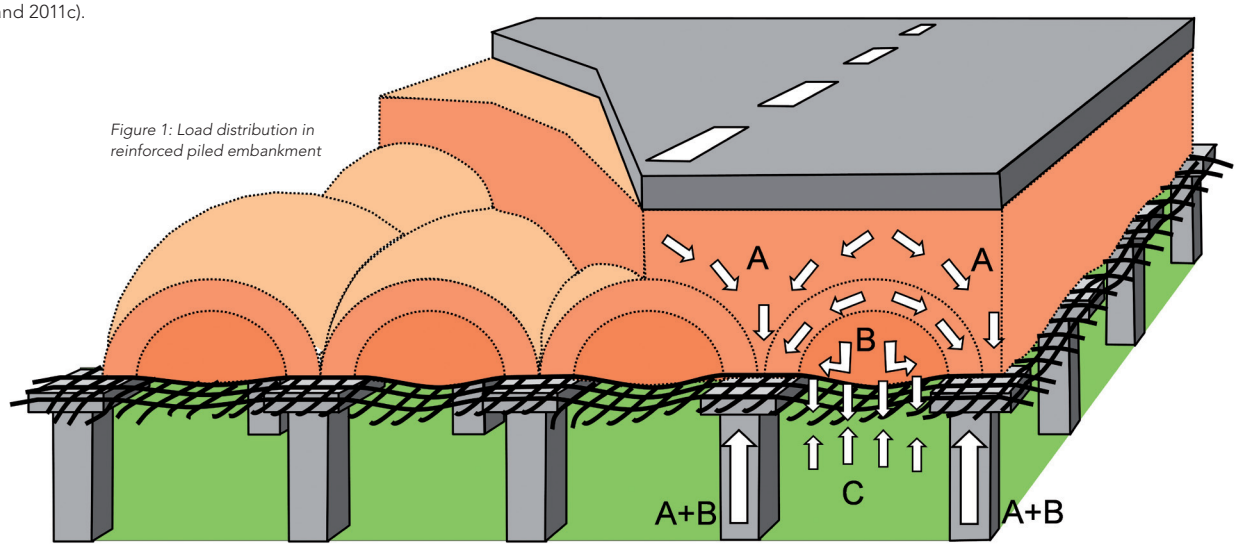

Figure 1: Load distribution in reinforced piled embankment

part C is carried by the soft subsoil. The load parts are vertical loads and are given in kN/pile.

Scale tests

A section of an embankment is modelled in a metal box of 1.1 x 1.1 x 1 m^3. Four piles are situated on the bottom of the box. The soft subsoil between the piles is modelled with a watertight foam cushion filled with water. A tap allows drainage from the foam cushion during the test, which models the consolidation process of the soft subsoil. The GR is attached to a steel frame and situated on top of the foam cushion with a sand layer of ca. 2 cm in between. On top of the GR, an embankment of 0.42 m is constructed of granular material (crushed rubble). The top load on the embankment is applied with a water cushion. This provides an equally distributed top load. The metal box is closed by a cover and tie rods. A side and top view of the scale test set-up is given in figure 2.

The scale tests are performed in several steps of consolidation by draining the foam cushion and increasing top load. The load steps and consolidation steps alternate: each top load step is followed by ca. 3 consolidation steps. At the end of the scale test, vacuum pressure is applied to the foam cushion. This reduces the subsoil support to zero. After every drainage or top load step, the system is allowed to stabilise for several hours. The load distribution is measured with pressure cells. Pressure cells are placed on top of piles, one above and one underneath the GR. The pressure cell above the GR measures load part A and the pressure cell underneath the GR measures load parts A+B. Load part B is calculated by subtracting load part A from load parts A+B. Additionally, the pressure in the foam cushion is measured, which gives load part C. The top load is measured with a water pressure meter in the water cushion. The vertical deformation of the GR is measured on three locations with a liquid levelling system. The locations of the measurements are given in figure 2.

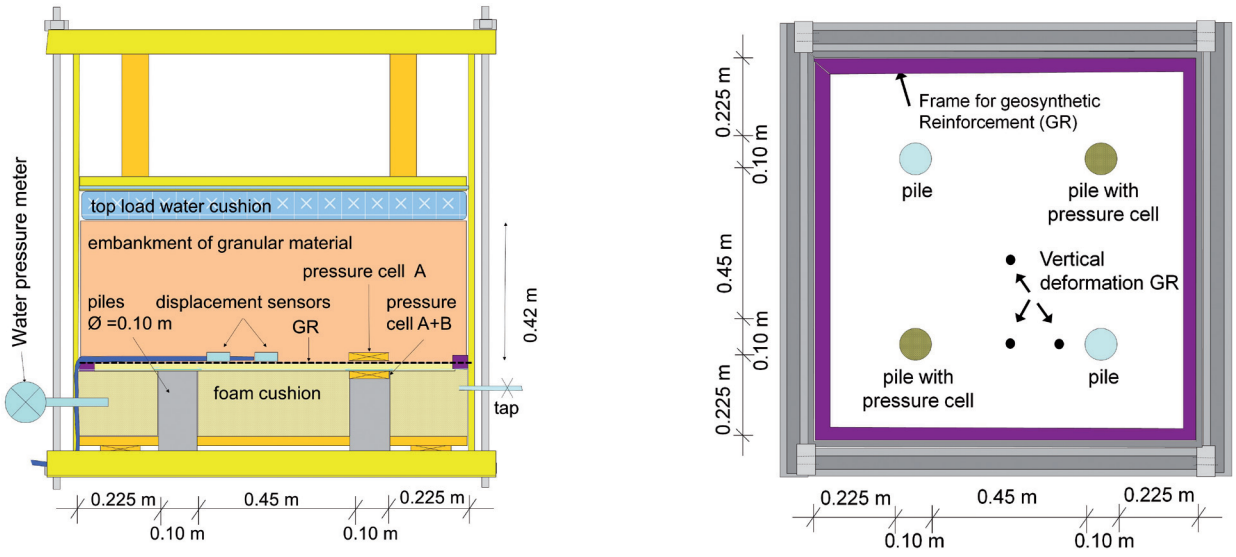

Figure 2: Side view and top view of scale test set-up

Finite element model

The scale tests are simulated with 3DTunnel version 2.4. 3DTunnel was used, because updated mesh could be applied and arching in the embankment is a 3D problem. Updated mesh is necessary to use, because the function of the GR depends on the deformation and the tension force cannot be modelled if the deformation is not captured in the calculation. The updated mesh function captures the tensile strains in the geosynthetic elements and the geosynthetic is no longer horizontal. Next to that the new PLAXIS 3D version was not available at the time. The geometry of the model is based on the geometry of the scale test. Because the geometry of the scale test is symmetric, one quarter of the scale test, one pile with surrounding soil, is modelled. The boundary conditions are horizontally fixed. The side and top view of the model are presented in figure 3. The material properties are summarized in table 1 and 2 and will be described in the next section.

In the test series, circular piles are applied. For the Plaxis simulations, the geometry of the circular pile is converted to a square pile. The properties of the pile are based on the parameters of PVC. PVC is modelled linear elastic and non-porous material. Next to the pile the foam cushion is modelled. The watertight and soaked foam cushion behaves linear elastic in the scale test. The scale tests were controlled by both top load and draining the foam cushion and therefore decreasing the water pressure in the foam cushion. To simulate the drainage of the scale test, the measured water pressure is prescribed in the model by applying a phreatic level to the clusters of the foam cushion. Therefore the measured water pressure is converted into a pressure head.

The axial stiffness of the GR is determined from five tensile tests. The tensile tests are performed according to DIN EN ISO 10319. The GR is attached to a steel frame. The steel frame is modelled, the weight of the frame disturbs the load distribution. The parameters of the steel frame are based on the properties of steel.

The sand layer on the pile and foam cushion and the granular material are modelled with the Hardening Soil model. The parameters of the sand and granular material are determined with triaxial tests. The sand layer is split up in two parts, a part above the pile and a part directly on the subsoil. The parameters are different for both parts. The sand on top of the pile is expected to behave very stiff, because the sand on the pile will be clamped between the GR and the pile. Therefore, the sand on the pile will be compressed more and will have higher stiffness and strength properties. The sand on the subsoil will follow the settlements of the subsoil and geosynthetics. In figure 4 the 3D finite element mesh created by Plaxis is shown.

During the execution of the scale tests, part of the load is dissipated due to friction. The friction between the wall and the granular material is between 10% and 20%. Normally an interface is applied to model the friction. This interface should be applied along the box walls, which means at the left and back side of the model. In Plaxis 3D

Table 1: material properties of pile, subsoil, GR and frame (linear elastic)

	γ [kN/m^3]	E_{ref} [kN/m^2]	υ [-]	EA [kN/m]
Pile	13.6	2.9E6	0.0	-
Subsoil	10.2	10	0.2	-
GR	-	-	-	2269
Frame	70.5	2.1E8	0	-

Table 2: material properties of sand and granular material (Hardening Soil model)

	γ [kN/m^3]	c [kN/m^2]	ϕ [°]	Ψ [°]	E_{50}^{ref} [kN/m^2]	E_{oed}^{ref} [kN/m^2]	m [-]	E_{ur}^{ref} [kN/m^2]	υ_{ur} [-]	ρ^{ref} [kN/m^2]	R_f [-]
Sand above pile	20.1	1	40.9	10.9	51470	51470	0.5	154410	0.2	100	0.9
Sand next to pile	18.7	1	32.5	2.5	19660	19660	0.5	58980	0.2	100	0.9
Granular material	16.7	1	47.0	11.0	58870	58870	0.7	176610	0.2	100	0.9

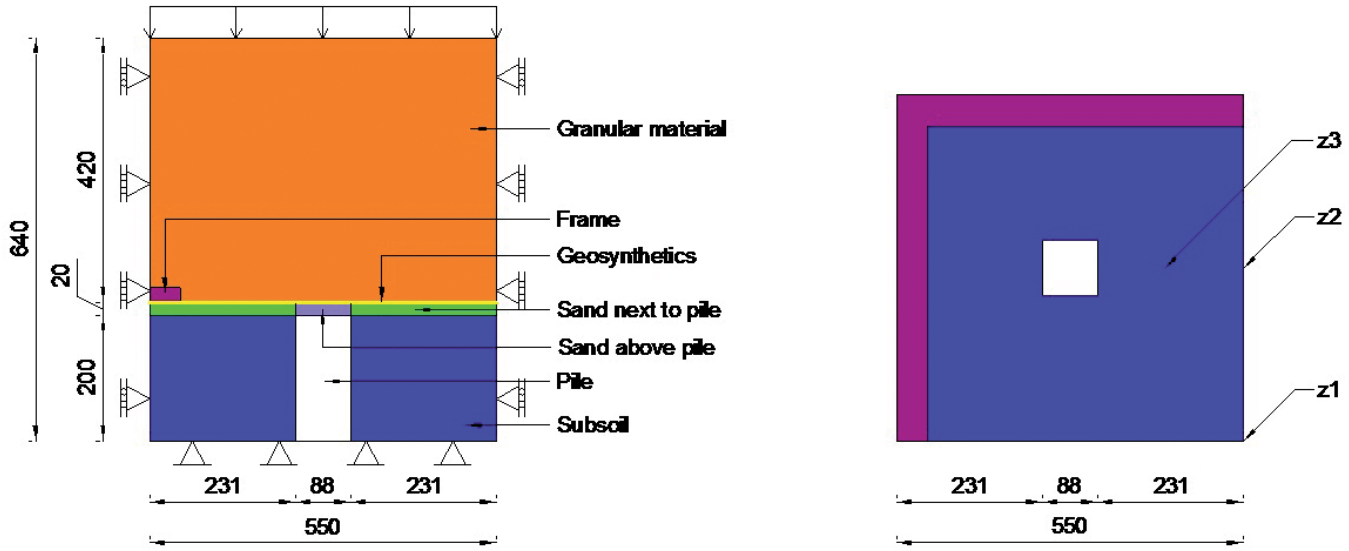

Figure 3: Top view and side view of finite element model

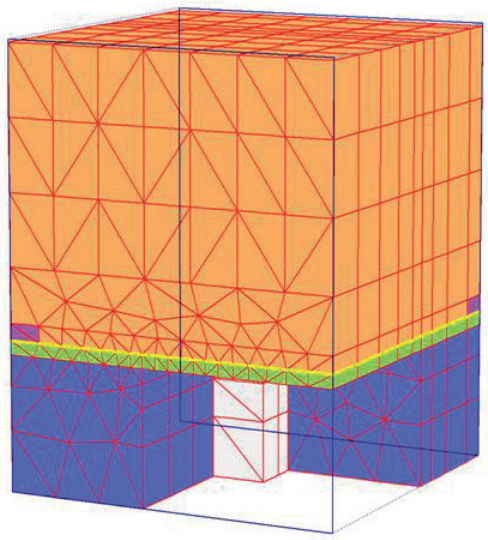

Figure 4: 3D finite element model

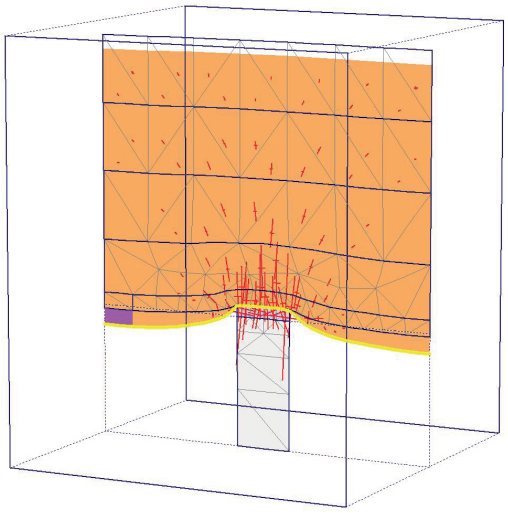

Figure 5: Effective principal stresses of the vacuum phase

Tunnel an interface cannot be applied at the back side. To keep the amount of load distribution comparable to the scale test, the top load is reduced by the amount of friction, and no interface is applied. The disturbance of the friction on the load distribution in the embankment is therefore neglected in the model. The friction between the piles and the foam cushion is assumed to be small and its influence on arching within the fill is limited. Therefore the friction between the pile and foam cushion is also neglected.

The calculation phases of the model are based on the scale test procedure. The top load and water pressure measured during each step of the scale test procedure is an input value in the calculation phases. During the initial phase, the water pressure and ΣMweight are set to zero, to avoid an asymmetric situation. In the following phases, the scale test is build up and the soil weight is activated. Then the measured load with corresponding water pressure is applied. During the last phase, where there is no subsoil support against the GR, the subsoil and water pressure are deactivated.

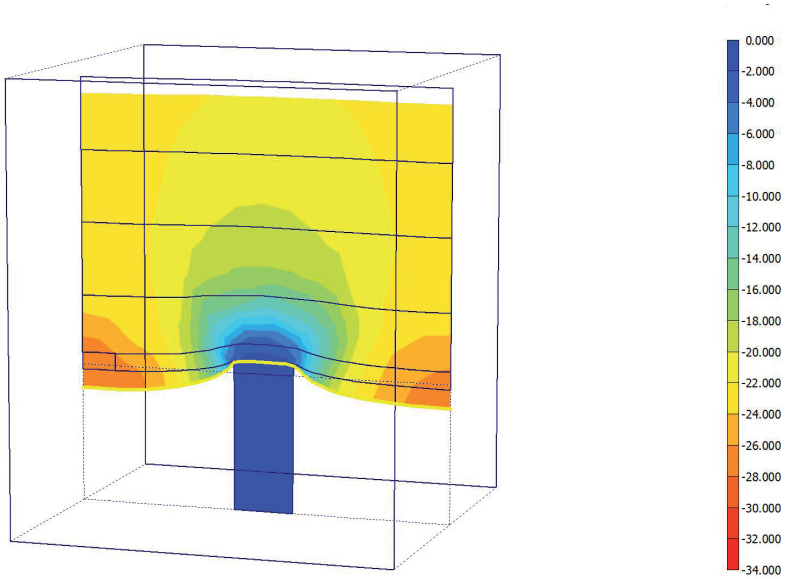

Figure 6: Vertical displacement of the vacuum phase

Results

During the vacuum phase there is a constant high top load applied and there is no subsoil support. Therefore, the vacuum phase has the largest deformation. This is the most representative situation and will be presented in the figures below. The calculated principal stresses in the vacuum phase are shown in figure 5. From the figure, soil arching can be observed. The calculated vertical displacements are shown in figure 6. The differential displacements on top of the embankment are very small. The tensile forces in the GR are presented in figure 7. The tensile forces in the GR are concentrated in 'tensile strips'. The tensile strips are the areas of that GR that lie on top of and between adjacent piles. The maximum tensile forces are found in the GR at the edge of the piles. The exact location of the peak values cannot be determined, because the mesh is too coarse.

The load distribution for the FEM model and the scale test are plotted in figure 8. The horizontal axis presents the net load. The net load is the top load minus subsoil support and friction. Load parts A and B are presented on the vertical axis in kN per pile and as percentage of the total load (A+B+C). The figures show two types of loading: top load increase and drainage of subsoil (consolidation). The load transferred directly to the piles due to arching is load A and the load transferred through the GR to the piles is load B. During the first part of the test, until the net load is ca.11 kN/pile, the calculated results of load parts A and B agree quite well with the measured results. Then the calculated results diverge from the measured results. Load part A is overestimated and load part B is underestimated. The calculated load parts A and B show a smooth relationship with the net load. This agrees with the conclusion of the measurements. During the first drainage step with zero top load, the percentage of load part A (A %) increases significantly. This means that arching occurs immediately. Not only during the first drainage step, but also in the following drainage steps load part A % increases. This shows that subsoil settlement is needed for the development of arching. This conclusion can be drawn for both the measured and calculated results. During the steps with increasing top load, load part A % on the embankment decreases. From this it follows that during increasing top load the arching effect decreases, as long as consolidation does not occur.

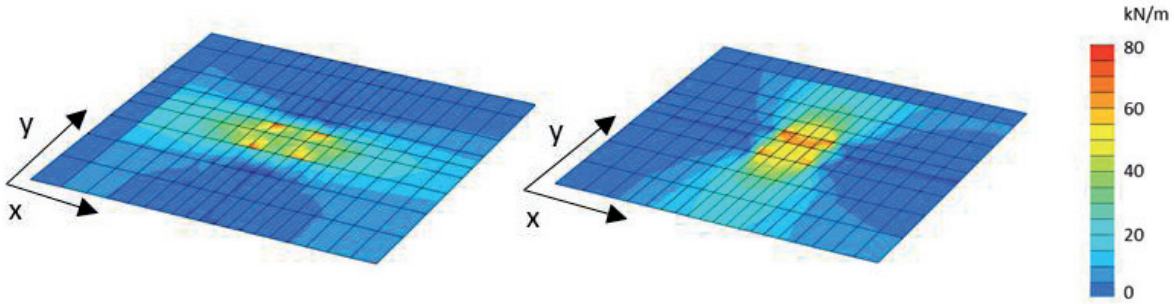

Figure 7: Tensile forces in GR of vacuum phase in x-direction (left) and in y- direction (right)

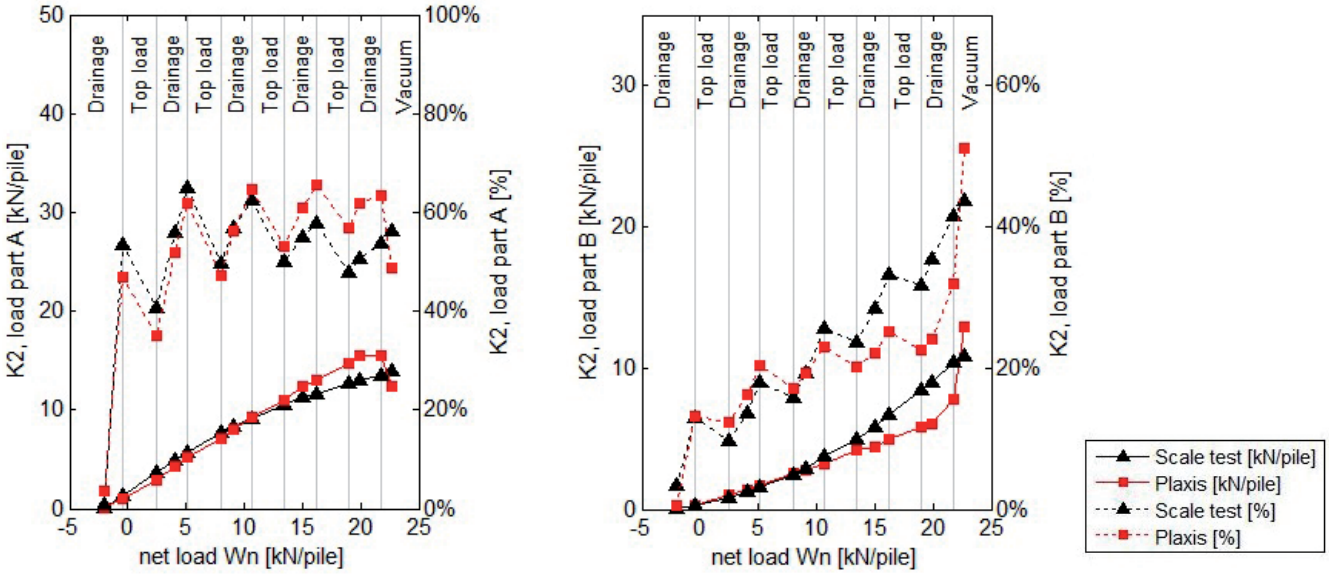

Figure 8: Load part A and B in kN/pile and in % of total load A+B+C

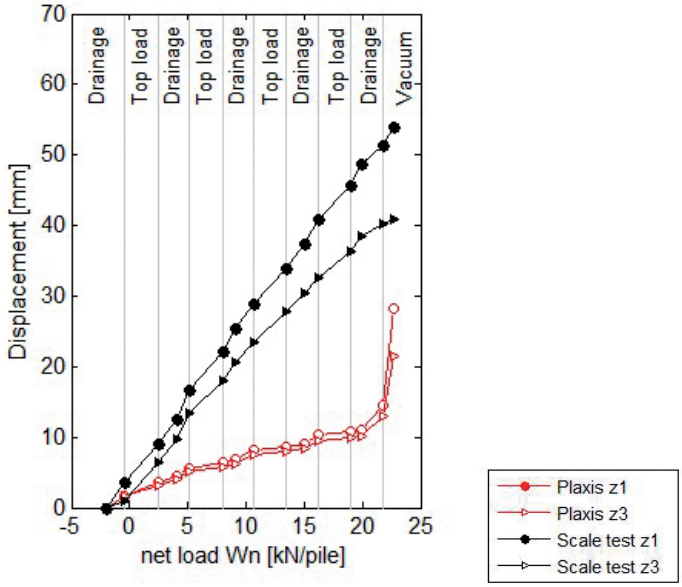

Figure 9: Displacement

Displacements have been measured at three places: in the middle of four piles (z1), in the middle of two piles (z2) and close to a pile (z3). Displacements z1 and z3 are shown in figure 9. Displacement z2 is not shown, because this displacement does not differ from displacement z3. The displacement is presented as a function of the net load. From the comparison of results between Plaxis and the measurements it can be concluded that the displacement is underestimated significantly by Plaxis. Farag (2008) also found much lower settlements in his Plaxis calculations. In CUR 226 (2010) this is solved by modelling a gap underneath the GR in the Plaxis calculations.

Several possible causes of the underestimated displacements have been investigated: among them the behaviour of the subsoil, of the GR and of the granular material. Each individual aspect gives a very limited improvement conform the measured displacements. Therefore, the cause of the underestimated displacements should be investigated in more detail.

Conclusions and recommendations

From the FEM model is concluded that arching occurs in the granular material. The effective vertical stresses are concentrated on top and the area next to the piles. The tensile forces in the GR are concentrated in 'tensile strips' between the piles. The exact location of the greatest tensile forces could not be determined because of the coarseness of the mesh.

In accordance with the measurements, Plaxis calculations give a smooth relationship between the net load and load parts A and B, and the GR settlements. During the first part of the test, the load distribution of the model agrees quite well with the measured load distribution. During the second part of the test, the load transferred through arching is overestimated and the load transferred through the GR is underestimated. In general, Plaxis finds an increasing arch during drainage of the subsoil (consolidation), this is in agreement with the measurements. The displacements calculated with Plaxis are underestimated compared to the scale test results. However, the largest displacement of the GR is found at the middle of four piles.

To increase the accuracy of the Plaxis results, the model should be calculated with a more refined mesh. The loss of load (due to friction) during the scale test is an important part of the scale test. It produces disturbance in the load distribution of the granular material. The friction should be included in the Plaxis model by an interface, therefore it is advised to perform numerical analysis of the scale model test with the full 3D version of Plaxis. The cause of the differences in calculated and measured displacement of the GR has to be investigated in more detail.

References

- CUR 226, 2010, Ontwerprichtlijn paalmatrassystemen ISBN 978-90-376-0518-1 (in Dutch)
- Den Boogert, T.J.M., 2011. Piled embankments with geosynthetic reinforcement, Numerical analysis of scale model tests, Master of Science thesis, Delft University of Technology.
- Van Eekelen, S.J.M., Bezuijen, A., Lodder, H.-J. & Van Tol, A.F., 2011a. Model experiments on piled embankments Part I, Geotextiles and Geomembranes, 2011, http://dx.doi.org/10.1016/j.geotexmem.2011.11.002
- Van Eekelen, S.J.M., Lodder, H.J., Bezuijen, A., 2011b, Paalmatrasproeven I, Vervormingen van geokunststoffen in een paalmatras en de daaruit volgende belastingsverdeling, GeoKunst 42, april 2011, 42-44
- Van Eekelen, S.J.M., Van der Vegt, J.W.G., Lodder, H.J., Bezuijen, A., 2011c, Paalmatrasproeven II, belangrijkste conclusies, GeoKunst 43, juli 2011, pp 46-50